Available online at www.sciencedirect.com

ScienceDirect

Scripta Materialia 61 (2009) 737–740

Scripta MATERIALIA

www.elsevier.com/locate/scriptamat

Electron channeling contrast imaging of twins and dislocations in twinning-induced plasticity steels under controlled diffraction conditions in a scanning electron microscope

I. Gutierrez-Urrutia,* S. Zaefferer and D. Raabe

Max-Planck-Institut für Eisenforschung, Max-Planck Str. 1, D-40237 Düsseldorf, Germany

Received 12 May 2009; revised 10 June 2009; accepted 12 June 2009
Available online 17 June 2009

Dislocation cells and mechanical twins have been imaged by electron channeling contrast imaging (ECCI) in a scanning electron microscope under controlled diffraction conditions in a deformed Fe–22Mn–0.6C twinning-induced plasticity (TWIP) steel using a novel set-up. The approach uses electron backscattered diffraction for orientation-optimized ECCI with enhanced dislocation and interface contrast. The observations provide new insights into the strain-hardening mechanisms of TWIP steels.
© 2009 Acta Materialia Inc. Published by Elsevier Ltd. All rights reserved.

Keywords: Scanning electron microscopy (SEM); Electron backscattering diffraction (EBSD); Austenitic steels; Dislocations; Twinning

Twinning-induced plasticity (TWIP) steels are promising materials for structural applications with excellent mechanical properties combining high strength (ultimate tensile strength of 700 MPa) and ductility (elongation to failure of 95%) due to high strain hardening [1–3]. The strain-hardening rate is attributed to the reduction of the dislocation mean free path with mechanical twins acting as obstacles to dislocation glide [1,4,5]. Mechanical twins in TWIP steels are extremely thin (~50 nm thick), and hence are generally studied by transmission electron microscopy (TEM) [1,4]. However, TEM is limited when it comes to the quantitative microstructural characterization of highly heterogeneous microstructures, such as encountered in deformed TWIP steels. Another microscopy technique for characterizing deformed microstructures is electron channeling contrast imaging (ECCI). ECCI is a scanning electron microscopy (SEM) technique that makes use of the fact that the backscattered electron intensity is strongly dependent on the orientation of the crystal lattice planes with respect to the incident electron beam due to the electron channeling mechanism [6–9]. Slight local distortions in the crystal lattice due to dislocations cause a modulation of the backscattered electron intensity, allowing the defect to be imaged. The ECCI technique has been used to image dislocation structures in metals deformed during fatigue [10,11] or associated with cracks [12,13]. For quantitative characterization of dislocation structures (e.g. Burgers vector analysis) and to image these structures with optimal contrast, it is required to conduct ECCI under well-controlled diffraction conditions as dislocation imaging is obtained by orienting the crystal matrix exactly into Bragg condition for a selected set of diffracting lattice planes. To date the only method utilized for performing ECCI of dislocations under controlled diffraction conditions is based on electron channeling patterns (ECPs) [8,9,14,15]. The main drawback of this technique is the requirement of a large final aperture to allow the beam to cover a large angular regime, leading to very low spatial resolution (above 2 μm [8], almost two orders of magnitude above the resolution of electron backscattered diffraction (EBSD)). This shortcoming reduces its application to the imaging of dislocation structures in lightly deformed metals. This also explains the limited number of works on the use of ECCI for imaging dislocation structures. In this paper, we present a novel set-up for the ECCI technique under controlled diffraction conditions where the crystal orientation is obtained by means of EBSD. This set-up provides an efficient and fast means to perform ECCI of dislocations under controlled diffraction conditions with enhanced dislocation and interface contrast. Further, we demonstrate that the ECCI technique can image dislocation cells and mechanical twins in a deformed TWIP steel by means of SEM.

* Corresponding author. Tel.: +49 2116792 211; fax: +49 211 6792 333; e-mail: i.gutierrez@mpie.de

1359-6462/$ - see front matter © 2009 Acta Materialia Inc. Published by Elsevier Ltd. All rights reserved.
doi:10.1016/j.scriptamat.2009.06.018

The material used in this study was a Fe–22Mn–0.6C (wt.%) TWIP steel. The material was melted in an induction furnace under an Ar atmosphere and cast into round bars 25 mm in diameter. Homogenized and hot-rolled samples (rolling temperature of 700 °C) were tensile deformed at room temperature to a strain of 0.2. ECCI of the deformed microstructures was performed using a dual-beam Zeiss-Crossbeam instrument (Carl Zeiss SMT AG, Germany) consisting of a Gemini-type field emission gun (FEG) electron column and an focused ion beam (FIB) device (Orsay Physics). This instrument is equipped with an EBSD system (EDAX/TSL, Draper, UT, USA). Dislocation structures and mechanical twins observed by ECCI were verified by transmission electron microscopy (TEM) using a Philips CM20 instrument. Thin foils of areas previously analyzed by ECCI were prepared by ion milling by means of FIB.

Figure 1a shows the schematic illustration of the new set-up proposed for ECCI under controlled diffraction conditions. The key point introduced here is to use EBSD instead of ECPs to orientate the crystal into optimal diffraction conditions. This allows the imaging of deformed microstructures with the most favorable electron channeling contrast even in highly deformed materials because of the much higher spatial resolution of EBSD (30 – 50 nm [16]) compared to ECP (2 μm [8]). The set-up comprises two sample positions: one for performing ECCI using a low-tilt configuration, where the sample is positioned perpendicular to the incident electron beam (ECCI position); and another one for performing EBSD measurements using a high-tilt configuration, where the sample is tilted 20° from the incident electron beam using a conventional EBSD geometry (EBSD position). A low-tilt configuration is selected for ECCI (ECCI position) because of the convenient position for performing crystal orientation experiments and the enhanced electron channeling contrast [17]. Furthermore, in the present configuration the lateral resolution is isotropic, in contrast to a high-tilt configuration, such as the EBSD position adapted by Ref. [18], where the lateral resolution is different for the tilted and the horizontal directions. In this configuration a small working distance is used (5–7 mm) to increase the amount of backscatter electrons collected by the detector, and hence to enhance the contrast. In this set-up the ECCI of dislocations under controlled diffraction conditions is performed as follows. The sample is turned into the ECCI position and the area for ECCI of dislocations is selected. Then the sample is tilted into the EBSD position and an EBSD map of the selected area or an individual orientation measurement is performed. Based on the determined crystal orientation, diffraction patterns of the selected area at the ECCI position are calculated using computer software [19] which provides the tilt and rotation angles required for orienting the crystal into optimal diffraction conditions.

The practice of creating and using controlled diffraction conditions is illustrated and explained in Figure 1b–d. Figure 1b shows the ECCI of a mechanical twin of 50 nm thickness in a tensile deformed Fe–22Mn–0.6C TWIP steel. Diffraction patterns of the crystal matrix and the twin are simulated by software [19] from the corresponding EBSD map. Diffraction conditions are selected for twin imaging with optimal contrast. This is achieved when one of the two crystals (matrix or twin) is oriented exactly in the Bragg condition for a high-intensity reflection and the other crystal is in an out-of-Bragg orientation. In the first case electrons are more effectively channeled into the lattice and the backscattering yield is low, making the crystal appear dark, whereas in the second case the backscattering yield is enhanced and the crystal appears bright. In this example, diffraction conditions are selected to image the matrix bright

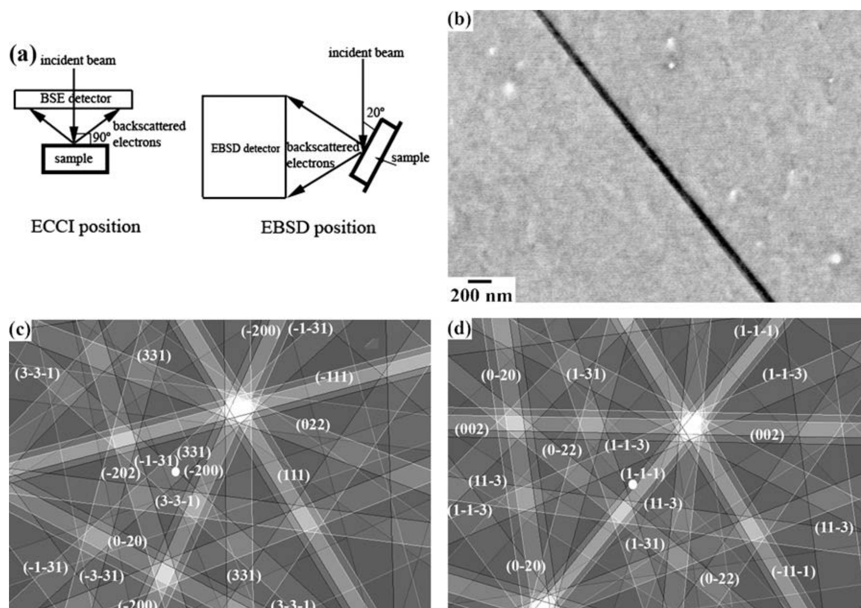

Figure 1. (a) Schematic illustration of the set-up for ECCI in SEM under controlled diffraction conditions. (b) ECCI of a mechanical twin under controlled diffraction conditions with the matrix bright and the twin dark. Simulated diffraction patterns of the crystal matrix (c) and twin (d).

(simulated diffraction pattern in Fig. 1c) and the twin dark using a high-intensity reflection of 111-type (simulated diffraction pattern in Fig. 1d). The rotation and tilt angles indicated by the software, 83° and 16°, respectively, are subsequently transferred to the microscope for contrast-optimized ECCI (Fig. 1b).

For further optimization of the electron channeling contrast, in particular for dislocation structures, the influence of the accelerating voltage was studied. ECCI of dislocation arrangements in a deformed Fe–22Mn–0.6C TWIP steel was performed using the set-up described above at different acceleration voltages between 7.5 and 30 kV corresponding to the sensitivity of the backscatter detector. Figure 2 shows an example of the significant influence of the accelerating voltage on the electron channeling contrast of dislocations. In this figure ECCI of dislocation arrangements in the exact same area at 20 kV (Fig. 2a) and 10 kV (Fig. 2b) are shown. 20 kV corresponds to the most common operating condition used in previous works on ECCI of dislocations [9–14], and 10 kV corresponds to the accelerating voltage at which the optimum contrast is obtained in the present case. It can be seen that the electron channeling contrast of dislocations is much sharper at 10 kV, where details in the dislocation arrangements and single dislocations are clearly resolved. There are two reasons for the improved contrast with decreasing acceleration voltage. First, with decreasing voltage the cross-section for phonon scattering—which is responsible for the backscattering yield—is increased. As a consequence the bright parts in the image, i.e. dislocations, appear brighter while the dark parts maintain their low intensity. A second reason for the improved contrast is the reduced interaction volume. In a smaller volume the lattice strain shows smaller variations, thus diffraction conditions and contrast are better defined. Optimal

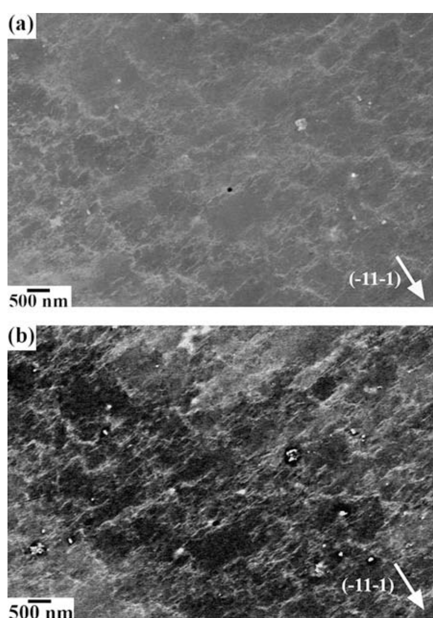

Figure 2. ECCI in SEM of dislocation arrangements in a tensile deformed Fe–22Mn–0.6C TWIP steel at two different accelerating voltages: (a) 20 kV and (b) 10 kV.

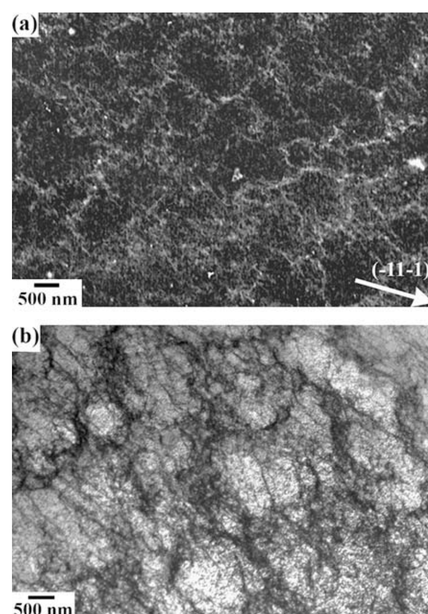

Figure 3. Dislocation cells in a tensile deformed Fe–22Mn–0.6C TWIP steel observed by (a) ECCI in SEM and (b) bright-field TEM of the same area.

ECCI is therefore obtained by operating at accelerating voltages below the commonly used value of 20 kV as this provides a much sharper electron channeling contrast of the dislocations.

Figure 3a shows ECCI of dislocation cells of around 1 μm average diameter in a tensile deformed Fe–22Mn–0.6C TWIP steel (0.2 strain). This is the first observation of dislocation cells in TWIP steels deformed at room temperature. Additionally, we demonstrate that this result can be obtained by SEM without the usual time-consuming TEM technique. The observation of dislocation cells in this material is not surprising as such cells have also been observed in materials with similar stacking fault energy, such as in stainless steel 316L [20]. However, as will be discussed below, this is an important finding for understanding strain-hardening mechanisms in this material. In order to confirm the dislocation structures observed by ECCI, a sample was first observed by ECCI under controlled diffraction conditions and the same area was cut out using a FIB, and prepared for TEM observations. Dislocation cells observed in the same area by ECCI in SEM and bright-field TEM are shown in Figure 3a and b, respectively. These figures demonstrate that both microscopy techniques reveal exactly the same structure, i.e. dislocation cells of around 1 μm average diameter. The ECCI technique also provides highly detailed images of the dislocation cell structure with the walls of cells clearly resolved and even single dislocations inside the cells distinguishable. The TEM image reveals that dislocation walls are formed by very few dislocations, confirming the capacity of the ECCI technique for resolving dislocation structures of very low misorientation with respect to the matrix.

Figure 4 shows ECCI of mechanical twins and dislocation cells under controlled diffraction conditions at low and high magnification. Figure 4b shows that extremely thin mechanical twins of 30 nm thickness can be

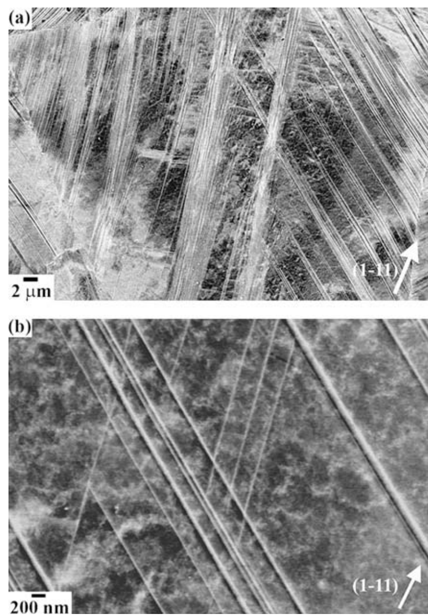

Figure 4. ECCI in SEM of dislocation cells and mechanical twins in a tensile deformed Fe–22Mn–0.6C TWIP at (a) low magnification and (b) high magnification.

clearly imaged by ECCI. Due to the sharp dislocation and interface contrast obtained by ECCI the interaction between mechanical twin boundaries and dislocation cells can be studied. Mechanical twins are seen to pass through dislocation cells, leading to the formation of new refined structures consisting of dislocation walls and mechanical twins. As the strain hardening is controlled by the dislocation mean free path [21], the size of these structures must also be considered. Thus, the dislocation mean free path is not only determined by the twin spacing, as is commonly considered [1,4,5], but also by the size of dislocation cells and the structures formed after the interaction of mechanical twins with the dislocation cells. The dislocation mean free path will be determined by different structural lengths depending on the strain level and the volume fraction of mechanical twins.

Figures 3a and 4 confirm that the ECCI technique is a powerful technique for characterizing deformed TWIP steels containing dislocation cells and mechanical twins by SEM. This is a significant advance in the microstructural characterization of deformed materials where these structures are typically observed by TEM [1,4,22]. As ECCI is a SEM technique it has the advantage over TEM that much larger areas can be observed, as shown in Figure 4a, and therefore quantitative microstructural characterization can be carried out, which is essential for understanding plasticity-related phenomena such as strain hardening. In addition, SEM samples are easier to prepare than TEM samples.

Dislocation cell structures and mechanical twins of 30 nm thickness have been imaged by ECCI in a tensile deformed Fe–22Mn–0.6C TWIP steel using a novel SEM–EBSD-based set-up. The observations provide new insights into strain hardening of TWIP steels and introduce the SEM-based ECCI technique as a powerful tool for characterizing highly deformed metals. The new set-up that we propose here provides an efficient and fast means to perform ECCI under controlled diffraction conditions in a conventional FEG scanning electron microscope equipped with an EBSD system.

The authors acknowledge the financial support by the German Research Foundation in the framework of SFB 761 "steel ab initio".

[1] O. Grässel, L. Krüger, G. Frommeyer, L.W. Meyer, Int. J. Plast. 16 (2000) 1391.
[2] G. Frommeyer, U. Brüx, P. Neumann, ISIJ Int. 43 (2003) 438.
[3] R. Ueji, N. Tsuchida, D. Terada, N. Tsuji, Y. Tanaka, A. Takemura, K. Kunishige, Scripta Mater. 59 (2008) 963.
[4] D. Barbier, N. Gey, S. Allain, N. Bozzolo, M. Humbert, Mater. Sci. Eng. A 500 (2009) 196.
[5] M.N. Shiekhelsouk, V. Favier, K. Inal, M. Cherkaoui, Int. J. Plast. 25 (2009) 105.
[6] E.M. Schulson, J. Mater. Sci. 12 (1977) 1071.
[7] D.C. Joy, D.E. Newbury, D.L. Davidson, J. Appl. Phys. 53 (1982) R81.
[8] A.J. Wilkinson, P.B. Hirsch, Micron 28 (1997) 279.
[9] M.A. Crimp, Microsc. Res. Tech. 69 (2006) 374.
[10] T. Zhai, J.W. Martin, G.A.D. Briggs, A.J. Wilkinson, Acta Mater. 44 (1996) 3477.
[11] Z.F. Zhang, Z.G. Wang, Z.M. Sun, Acta Mater. 49 (2001) 2875.
[12] B.C. Ng, B.A. Simkin, M.A. Crimp, Ultramicroscopy 75 (1998) 137.
[13] Y. Kaneko, M. Ishikawa, S. Hashimoto, Mater. Sci. Eng. A 400–401 (2005) 418.
[14] M.A. Crimp, B.A. Simkin, B.C. Ng, Phil. Mag. Lett. 81 (2001) 833.
[15] P. Morin, M. Pitaval, D. Besnard, G. Fontaine, Phil. Mag. A 40 (1979) 511.
[16] S. Zaefferer, Ultramicroscopy 107 (2007) 254.
[17] B.A. Simkin, M.A. Crimp, Ultramicroscopy 77 (1999) 65.
[18] C. Trager-Cowan, F. Sweeney, P.W. Trimby, A.P. Day, A. Gholinia, N.H. Schmidt, P.J. Parbrook, A.J. Wilkinson, I.M. Watson, Phys. Rev. B 75 (2007) 085301.
[19] S. Zaefferer, J. Appl. Cryst. 33 (2000) 10.
[20] X. Feaugas, Acta Mater. 47 (1999) 3617.
[21] U.F. Kocks, H. Mecking, Prog. Mater. Sci. 48 (2003) 171.
[22] J.G. Sevillano, P. Van Houtte, E. Aernoudt, Prog. Mater. Sci. 25 (1980) 69.